

Selective Removal of 3-Chlorophenol from Aqueous Solution Using Surface Molecularly Imprinted Microspheres

Xue Wang,[†] Jianming Pan,[†] Wei Guan,[†] Jiangdong Dai,[†] Xiaohua Zou,[†] Yongsheng Yan,^{*,†} Chunxiang Li,[†] and Wei Hu^{†,‡}[†]College of Chemistry and Chemical Engineering, Jiangsu University, Zhenjiang 212013, China[‡]School of Material Science and Engineering, Jiangsu University of Science and Technology, Zhenjiang 212003, China

ABSTRACT: A simple method for selective recognition of 3-chlorophenol (3-CP) from aqueous solution has been developed using a surface molecularly imprinted polymer (MIP) as sorbent. Characterization of the obtained MIP was achieved by Fourier transform infrared spectroscopy (FTIR). Kinetic, thermodynamic, dynamic adsorption, and selectivity experiments were investigated in this study. Kinetic experimental data were well-described by the pseudosecond-order kinetic model. The obtained Arrhenius activation energy E_a from the kinetic data indicated a physisorption mechanism, and the negative values of ΔH° demonstrated that the adsorption of 3-CP onto MIP was exothermic. Equilibrium experimental data of MIP fitted the Langmuir isotherm well. The MIP showed outstanding affinity toward 3-CP in aqueous solution, and the optimum pH value for binding has been found around the neutral range. When methanol was used as eluent, the adsorbed 3-CP eluted easily from MIP. The total dynamic capacity of the imprinted sorbent was calculated to be $1137.58 \text{ mg} \cdot \text{g}^{-1}$. The breakthrough of 3-CP started after 60 mL, and the breakthrough capacity was $756.8 \text{ mg} \cdot \text{g}^{-1}$. Meanwhile, selectivity experiments demonstrated that MIP showed high affinity to target molecules over competitive CPs (2,6-dichlorophenol and 2,4,6-trichlorophenol).

■ INTRODUCTION

Phenolic pollutants, such as chlorophenols (CPs), are very commonly used and have been highlighted as priority pollutants by the United States Environmental Protection Agency (EPA).¹ They are extensively used in chemicals, pharmaceuticals, petroleum, plastics, wood, rubber, herbicides, insecticides, and other industries.^{2,3} In addition, they can be directly or indirectly released into environmental systems. However, these phenolic components seriously affect both public health and environmental quality due to their high toxicity and accumulation in the environment, even though they have great commercial value.⁴ Meanwhile, considerable attention has been paid to the removal of phenolic pollutants from environmental systems. Physical, chemical, and biological methods, including incineration, adsorption on activated carbon, chemical or enzymatic oxidation, solvent extraction, microbial degradation, and others, have been used for removing or degrading several CPs from different water systems.⁵ However, it is difficult to achieve separation of trace amounts of target compounds from complex matrices directly without sample pretreatment. Hence, sample pretreatment for the quantitative determination of trace amounts of phenolic pollutants in environmental water is frequently required to attain enrichment.⁶

Selective separation technologies, such as liquid chromatography (LC) and gas chromatography (GC), are often used for the quantitative analysis of trace contaminants in environmental systems. Recently, among numerous new separation techniques, the molecular imprinting technique has received considerable attention as a new technique to synthesize materials capable of molecular recognition.⁷ Molecular imprinting is a convenient and powerful technique for the preparation of polymeric materials with special artificial recognition sites. These sites are

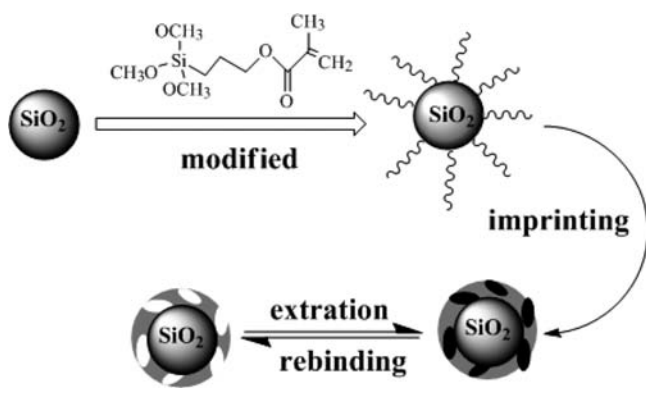
tailor-made by copolymerization of functional monomers and cross-linkers around the template molecules. Then, the printing molecules are subsequently removed from the polymer by elution using Soxhlet extraction, leaving special recognition binding sites in the polymeric network. So, those sites have special recognition properties for target molecule.⁸ The molecularly imprinted polymers (MIPs) prepared with conventional methods have some disadvantages, such that the number of recognition sites per unit volume of the polymer is relatively low. To overcome these drawbacks effectively, the surface molecular imprinting technique has been developed in recent years. The surface imprinting technique can be divided basically into two kinds: one is based on emulsion and precipitation polymerization, and the other is based on the surface modification of silica gel particles.⁹ Additionally, MIPs have been used for sample enrichment for the determination of a wide range of analyses, such as 2,4,6-trinitrotoluene,¹⁰ 2,4-dichlorophenol,¹¹ 4-nitrophenol,¹² bisphenol A,¹³ cinchonidine,¹⁴ β -estradiol,¹⁵ diclofenac,¹⁶ and corticosteroids.¹⁷ Solid-phase extraction (SPE) is routinely used for preconcentration and cleanup in the analysis of biological and environmental samples due to the advantages of simplicity, rapidness and little consumption of organic solvents. When MIPs are used as SPE media, it is desirable to prepare spherical and monodispersed beads. Molecularly imprinted solid-phase extraction (MISPE) provides a way to selectively enrich analytes which are present in low concentrations or in a complex matrix.¹⁸

Received: November 29, 2010

Accepted: April 20, 2011

Published: April 29, 2011

Scheme 1. Synthesis Route of the Surface Imprinted Polymer Sorbent



The aim of this study was to synthesize surface molecularly imprinted polymers using 3-chlorophenol (3-CP) as a template molecule, methacrylic acid (MAA), as a functional monomer and ethylene glycol dimethacrylate (EGDMA) as a cross-linker. The adsorption capacity was demonstrated by equilibrium batch experiments. The selectivity of the obtained materials was elucidated by performing adsorption experiments in mixed solution.

EXPERIMENTAL SECTION

Materials and Methods. EGDMA was obtained from the Aladdin Reagent Co. Ltd. (Shanghai, China). 2,2'-Azobisisobutyronitrile (AIBN) was purchased from the Shanghai No. 4 Reagent & H.V. Chemical Co. Ltd. (Shanghai, China) and recrystallized from methanol before use. Glycidoxypropyltrimethoxysilane (KH-570), MAA, and acetonitrile were all purchased from the Chemical Reagent Corporation (Shanghai, China). 3-CP, 2,4,6-trichlorophenol (2,4,6-TCP), and 2,6-dichlorophenol (2,6-DCP) were supplied by the Sinopharm Chemical Reagent Co. Ltd. (Shanghai, China). All chemicals were of analytical reagent grade, except for methanol which was of high-performance liquid chromatography (HPLC) grade. Deionized water was used throughout this study.

Stock standard solutions of 3-CP were freshly prepared in deionized water containing a little methanol and were stored in a refrigerator. All working solutions were prepared by diluting the stock standard solutions with doubly distilled water (DDW) to the needed concentrations.

Preparation of KH-570 Modified Silica Particles. KH-570 as a silane coupling agent was used to synthesize functionalized silica gel. For the preparation of silica nanoparticles (KH-570/SiO₂), 5.0 g of silica nanoparticles and 25 mL of KH-570 were added into 100 mL of anhydrous toluene in a three-necked flask. The mixture was refluxed for 12 h under nitrogen protection at 80 °C. After being separated by filtration and washed with ethanol, water, and toluene, respectively, the obtained sample was dried under vacuum at 60 °C for 24 h. Finally, the KH-570/SiO₂ nanoparticles were obtained.

Preparation of Imprinted and Nonimprinted Polymers. The synthesis route of the imprinting polymer sorbent is shown in Scheme 1. The synthesis of surface molecularly imprinted microspheres, in this study, was carried out by the following method: 3-CP (1.0 mmol), KH-570/SiO₂ composites (0.5 g),

and acetonitrile (10 mL) were transferred into a 25 mL flask. The mixture was magnetically mixed at 25 °C for 24 h to achieve prepolymerization. After being filtered, the saturated composites, MAA (6.0 mmol), EGDMA (6.9 mL), AIBN (0.15 g), and acetonitrile (12 mL) were added into a 25 mL flask. The flask was then sealed under nitrogen and placed in a water bath at 60 °C. Subsequently, the reaction was allowed to react for 24 h with stirring in a nitrogen atmosphere. After that, the obtained polymer was washed with the mixture solution of methanol/acetic acid (9:1, v/v) using Soxhlet extraction to remove the template molecules (3-CP). Finally, the obtained MIP was dried under vacuum at 60 °C for 24 h. Finally, MIP with a high affinity and excellent selectivity for 3-CP was prepared. In comparison, a nonimprinted polymer (NIP) without the template molecules (3-CP) was prepared in parallel with the MIP by using the same synthetic procedure.

Adsorption Experiments. The effect of experimental parameters such as pH, contact time, and temperature on the removal of 3-CP was studied by batch mode experiment. To study the effect of pH on the removal of 3-CP from aqueous solutions, 0.05 g of MIP was dispersed in 25 mL of solution containing 3-CP (100 mg · L⁻¹) at 25 °C for 12 h. The initial pH value of the solution was adjusted from 2.0 to 11 by using a certain amount of dilute HCl or NaOH solution.

Batch adsorption experiments were carried out by allowing a weighed amount of polymer to reach equilibrium with 3-CP solution of known concentration. For this purpose, 0.01 g of MIP was dispersed in 10 mL of 3-CP solutions at different concentrations (from 20 mg · L⁻¹ to 500 mg · L⁻¹). Then the suspensions were sealed and oscillated for 24 h at constant temperatures of 25 °C, 35 °C, and 45 °C, with pH = 7.0. At the end of the desired equilibrium period, the solution were centrifuged for 10 min, and the residual concentration of 3-CP in the aqueous solution after equilibrium adsorption was determined by UV-vis spectrophotometry (model UV-2450, Shimadzu Corporation, Japan) at 275 nm. Batch kinetic studies were identical to the adsorption experiments, but the aqueous samples were taken at prespecified time intervals.

The amount of adsorption at equilibrium Q_e (mg · g⁻¹) was calculated by the following equation:

$$Q_e = \frac{(C_0 - C_e)V}{W} \quad (1)$$

where C_0 and C_e represent the initial and equilibrium 3-CP concentrations in the solution (mg · L⁻¹), respectively; V is the volume of the solution (mL), and W is the amount of sorbent (mg).

Selectivity Studies. To determine the binding selectivity of MIP microspheres for 3-CP, 2,4-DCP, and 2,4,6-TCP were selected as interfering molecules since their molecular structures are quite similar to 3-CP. Briefly, MIP (0.02 g) was dispersed in 10 mL (100 mg · L⁻¹) solutions containing 3-CP, 2,4-DCP, and 2,4,6-TCP. The pH values of the solution were adjusted appropriately, and the mixtures were shaken in thermostatically controlled water at 25 °C for 24 h. The concentration of the mixture was determined by HPLC. The distribution coefficients (K_d), selectivity coefficients (k), and relative selectivity coefficient (k') of 3-CP, 2,4,6-TCP, and 2,6-DCP can be obtained according to eqs 2 to 4.

$$K_d = \frac{Q_e}{C_e} \quad (2)$$

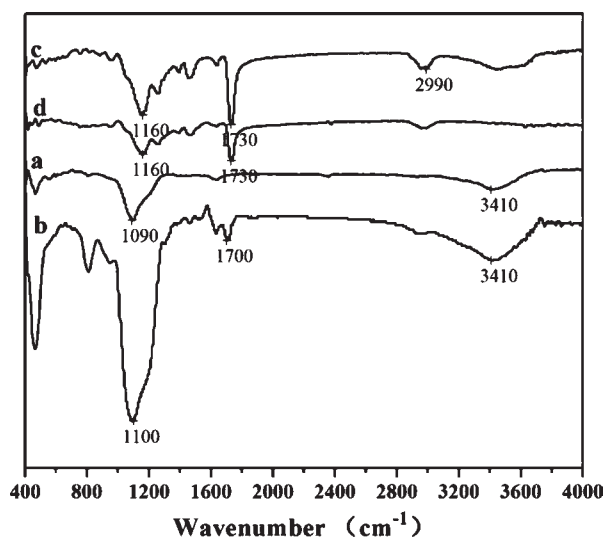


Figure 1. FTIR spectra of (a) SiO₂, (b) KH-570/SiO₂, (c) MIP, and (d) NIP.

where K_d represents the distribution coefficient ($L \cdot g^{-1}$); Q_e ($mg \cdot g^{-1}$) is the equilibrium adsorption capacity; C_e ($mg \cdot L^{-1}$) is the equilibrium concentration.

The selectivity coefficient of MIP for 3-CP with respect to the competitor species can be obtained from the equilibrium binding data according to:

$$k = \frac{K_{d(3-CP)}}{K_{d(X)}} \quad (3)$$

where k is the selectivity coefficient and X represents the competitive molecules. The relative selectivity coefficient k' defined in eq 4 indicates the enhanced extent of adsorption affinity and selectivity of MIP for the template. k_M and k_N are the selectivity coefficients of MIP and NIP, respectively.

$$k' = \frac{k_{MIP}}{k_{NIP}} \quad (4)$$

Dynamic Adsorption Procedure. The process of the dynamic experiment was conducted as follows. Briefly, MIP (0.5 g) was packed into a glass column and rinsed with acetonitrile, ethanol, and then with the loading solvent. Then a 3-CP standard solution ($1.0 g \cdot L^{-1}$) was passed through the column at room temperature after adjusting the appropriate pH at a flow rate of $1.0 mL \cdot min^{-1}$. After that, vacuum was applied for a few minutes to remove residual solvent. Washing solvent was then passed through the column, and finally, after column drying, elution solvent (5 mL methanol) was applied to perform the complete extraction of 3-CP molecules at a flow rate of $0.5 mL \cdot min^{-1}$ throughout the process. The concentration of 3-CP in the effluent liquid and the eluent was determined by UV-vis spectrophotometry (model UV-2450, Shimadzu Corporation, Japan) at 275 nm. In addition, before being packed into the glass column, MIP composites were dispersing in 20 mL DDW for a few hours at room temperature to achieve full swelling, and this was carried out three times.

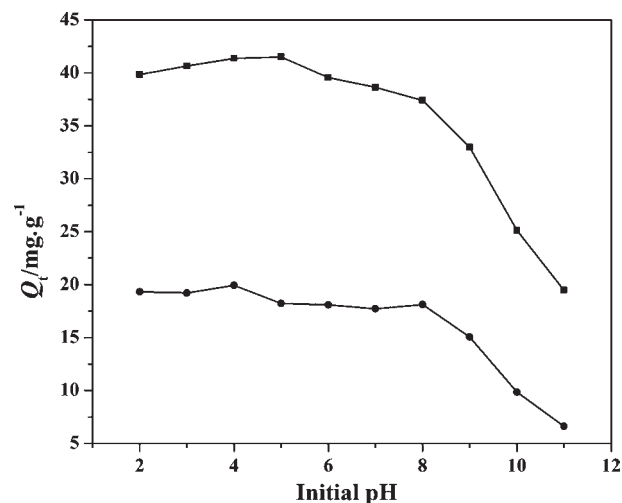


Figure 2. Effect of initial pH on the adsorption of 3-CP onto MIP and NIP. ●, NIP; ■, MIP; $T = 298 K$, $m = 0.05 g$, $V = 25 mL$, contact time = 24 h.

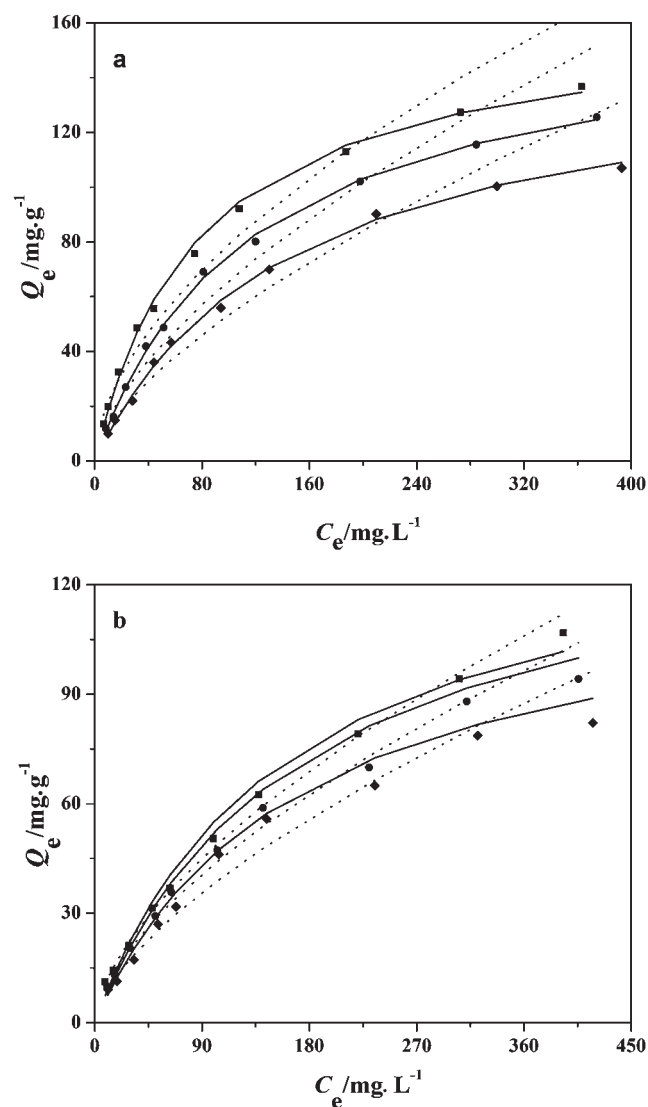
RESULTS AND DISCUSSION

Characterization of Sorbents. To identify the characteristic functional groups present in (a) SiO₂, (b) KH-570/SiO₂, (c) MIP, and (d) NIP and provide evidence for modification achieved through KH-570/SiO₂ treatment, FTIR analysis has been conducted, as shown in Figure 1. In the SiO₂ spectrum, it is possible to observe a strong Si–O band centered at $1090 cm^{-1}$, and this characteristic peak can be found in KH-570/SiO₂, MIP, and NIP. After modification and polymerization, it has shifted to $1100 cm^{-1}$ (KH-570/SiO₂) and $1160 cm^{-1}$ (MIP and NIP) which may be due to the influence of other groups. With regard to KH-570/SiO₂, MIP, and NIP, it can be observed that a peak appeared at $1700 cm^{-1}$ and $1730 cm^{-1}$, which is the characteristic peak of the C=O stretching vibration, and this could be evidence of the successfully modified of SiO₂ by KH-570.

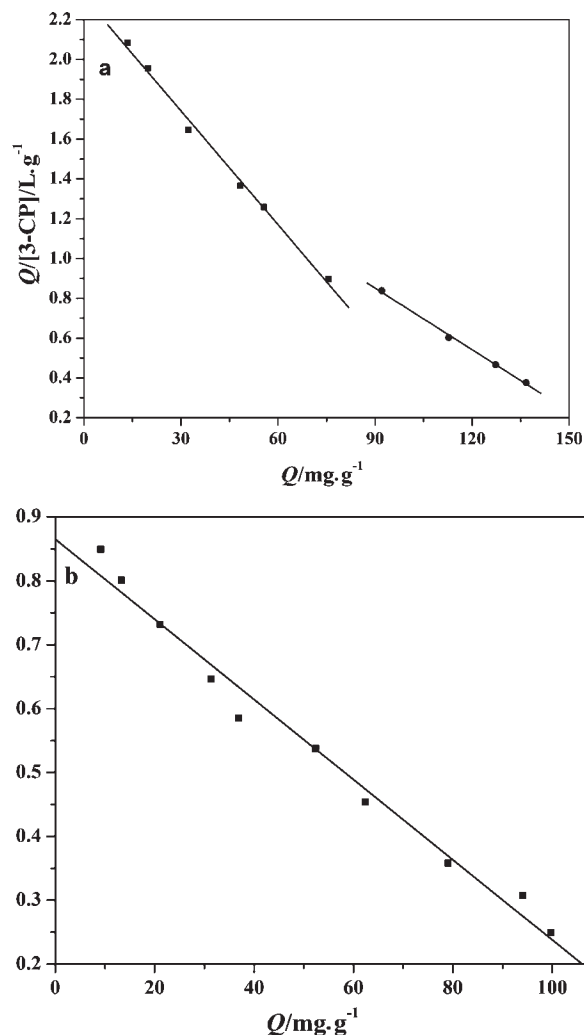
Effect of pH. The pH value of the solution is a most important factor affecting 3-CP adsorption onto the MIP and NIP. Figure 2 shows the effect of pH on the adsorption of 3-CP onto MIP and NIP. It was evident that the adsorption capacity is strongly influenced by the pH of the solution. As shown in Figure 2, adsorption efficiencies of 3-CP by MIP change very little at the beginning of adsorption but decrease significantly with the increase of pH, when the pH was between 8.0 and 11.0. The same trend was also observed in the NIP experiment. The possible reason for this can be attributed to the degree of ionization of phenol compounds as the solution pH changes and the organophilic nature of the sorbent surface. Obviously, 3-CP will be dissociated to $C_6H_5O^-$ when $pH > pK_a$ (3-CP is a weak acid, $pK_a = 9.96$), and this may influence the hydrogen bonding interaction and electrostatic effect between sorbent and the 3-CP molecules.¹⁹ At higher pH, the ionization degree of 3-CP and the quantity of OH^- ions increase, thereby the diffusion of 3-CP molecules are hindered. As a result, the removal of 3-CP is greater at lower pH compared to higher pH.²⁰ This demonstrated that the adsorption of 3-CP by MIP was in undissociated form. The experimental results make it clear that pH 7.0 was the optimum pH through this study. Such an

Table 1. Isotherm Constants for Adsorption of 3-CP onto MIP and NIP in Single Species Systems

adsorbent	T/K	Langmuir				Freundlich		
		Q_m $\text{mg}\cdot\text{g}^{-1}$	K_L $\text{L}\cdot\text{mg}^{-1}$	R_L	R^2	K_F $\text{mg}\cdot\text{g}^{-1}$	n	R^2
MIP	295	163.7	0.01276	0.1355	0.9959	5.815	1.763	0.9706
	305	163.6	0.00855	0.2253	0.9978	3.552	1.578	0.9728
	315	149.5	0.00687	0.1896	0.9958	2.580	1.520	0.9774
NIP	295	143.1	0.00626	0.2422	0.9637	2.792	1.618	0.9967
	305	142.8	0.00574	0.2583	0.9770	2.455	1.603	0.9935
	315	125.0	0.00560	0.2631	0.9835	1.932	1.543	0.9867

**Figure 3.** Nonlinear Langmuir and Freundlich isotherms for the adsorption of 3-CP onto: (a) MIP and (b) NIP in a single species system. ■, 25 °C; ●, 45 °C; ◆, 65 °C; —, Langmuir isotherm; ···, Freundlich isotherm. $m = 0.01$ g, $V = 10$ mL, $\text{pH} = 7.0$, contact time = 24 h.

adsorption property was favorable for 3-CP separation and detection from drinking water where the real pH value approaches 7.0.

**Figure 4.** Scatchard plot analysis of the adsorption of 3-CP onto (a) MIP and (b) NIP.

Adsorption Experiments. Adsorption isotherms are important in investigating how adsorbates interact with sorbents. The Langmuir isotherm and Freundlich isotherm are the two most widely used models to represent equilibrium data of adsorption. The Langmuir isotherm presupposes that the adsorption is on a monolayer. The Freundlich isotherm, on the other hand, is an empirical equation which assumes a heterogeneous surface energy. The nonlinear form of the Langmuir and Freundlich isotherm models are expressed by the following equations, respectively:²¹

$$Q_e = \frac{K_L Q_m C_e}{1 + K_L C_e} \quad (5)$$

$$Q_e = K_F C_e^{1/n} \quad (6)$$

where Q_e is the adsorbed amount of 3-CP ($\text{mg}\cdot\text{g}^{-1}$), C_e is the equilibrium concentration in the solution ($\text{mg}\cdot\text{L}^{-1}$), Q_m is the monolayer capacity of the sorbent ($\text{mg}\cdot\text{g}^{-1}$), K_L is the Langmuir adsorption constant ($\text{L}\cdot\text{mg}^{-1}$), K_F is the Freundlich constant ($\text{L}\cdot\text{g}^{-1}$), and $1/n$ is the heterogeneity factor.

The essential characteristics of the Langmuir isotherm can be expressed by a dimensionless constant called the equilibrium

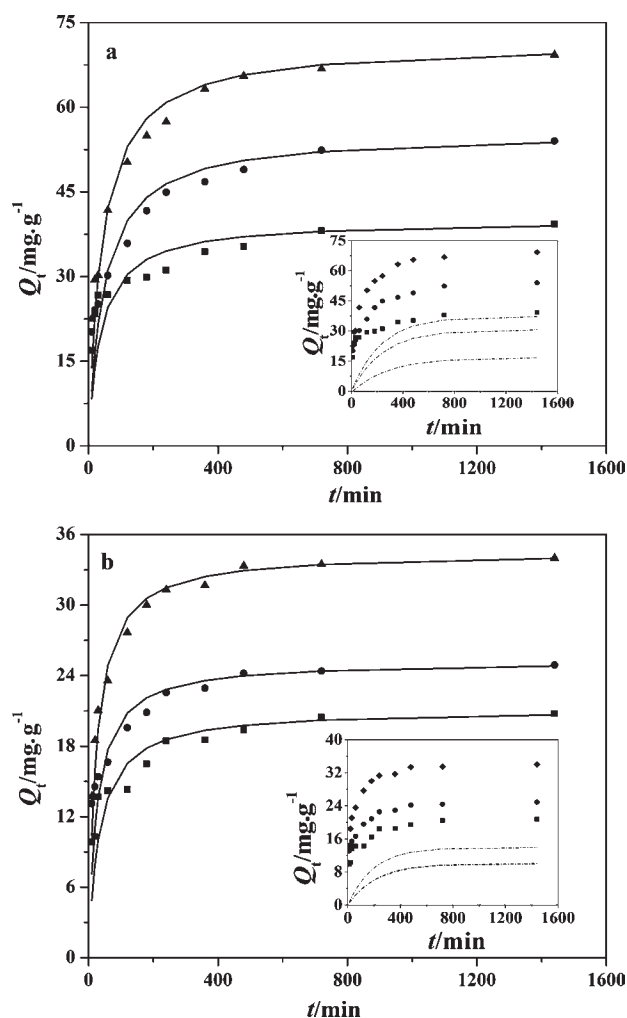


Figure 5. Kinetic modeling of the effect of 3-CP initial concentration on adsorption of 3-CP onto: (a) MIP and (b) NIP. ■, 100 mg·L⁻¹; ●, 150 mg·L⁻¹; ◆, 200 mg·L⁻¹. —, pseudo-second-order; ···, pseudo-first-order. $T = 298$ K, $m = 0.02$ g, $V = 5.0$ mL, pH = 7.0.

parameter, R_L , which is defined as:²²

$$R_L = \frac{1}{1 + C_m K_L} \quad (7)$$

where C_m is the maximal initial 3-CP concentration (mg·L⁻¹). There are four probabilities for the R_L value: (1) $0 < R_L < 1.0$, favorable adsorption; (2) $R_L > 1.0$, unfavorable adsorption; (3) $R_L = 1.0$, linear adsorption; (4) $R_L = 0$, irreversible adsorption. All of the calculated values of the adsorption experiment are listed in Table 1.

As can be seen from Figure 3, the adsorption capacity of 3-CP onto MIP and NIP decreases with increasing temperature, and the adsorption ability of MIP was better than NIP. The temperature increase from 25 °C to 45 °C results in a decrease in K_F values which demonstrates that the adsorption capacity was influenced by temperature. On the other hand, the R_L values (lying between 0 and 1.0) and the Freundlich constant n (higher than 1.0) shown in Table 1 indicate that the experiment conditions were favorable for 3-CP adsorption.²³ The calculated R^2 values in Table 1 and fitted adsorption isotherm in Figure 3 reflected that the adsorption of 3-CP onto MIP was

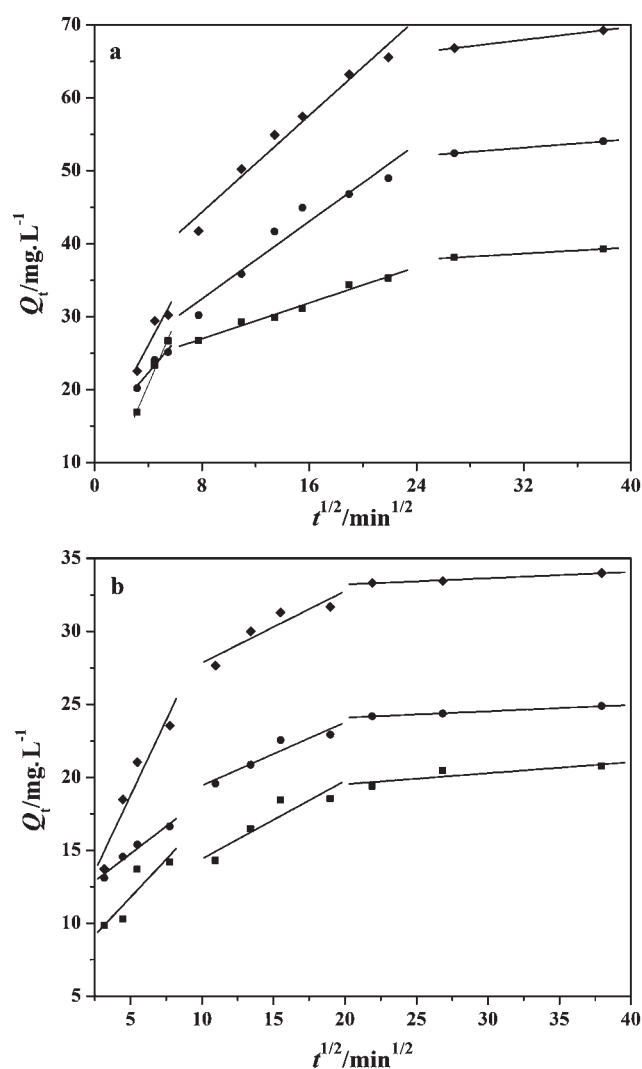


Figure 6. Intraparticle diffusion treatment of 3-CP onto (a) MIP and (b) NIP. ■, 100 mg·L⁻¹; ●, 150 mg·L⁻¹; ◆, 200 mg·L⁻¹. $C_0 = 100$ mg·L⁻¹, $m = 0.02$ g, $V = 5.0$ mL, solution pH: 7.0.

well-described by the Langmuir isotherm, but NIP was in good agreement with the Freundlich isotherm.

A Scatchard analysis was used for evaluation of the adsorption of MIP and NIP according to the following equation:²⁴

$$\frac{Q}{[3\text{-CP}]} = \frac{Q_{\max} - Q}{K_d} \quad (8)$$

where Q is the amount of 3-CP bound to the polymers at equilibrium; $[3\text{-CP}]$ is the free 3-CP concentration at equilibrium; K_d is the dissociation constant, and Q_{\max} is the apparent maximum binding amount. The values of K_d and Q_{\max} can be calculated from the slope and intercept of the linear plot of $Q/[3\text{-CP}]$ versus Q .

As shown in Figure 4a, the Scatchard plot for MIP was not a single linear curve but consisted of two linear parts with different slopes. In Figure 4a the linear regression equation for the left part of the curve was $Q/[3\text{-CP}] = -0.01905Q + 2.3128$. The K_d and Q_{\max} values were calculated to be 52.49 mg·L⁻¹ and 121.4 mg·g⁻¹ of dry polymer, respectively. The linear regression equation for the right part of this curve was $Q/[3\text{-CP}] = -0.01031Q + 1.7792$.

Table 2. Kinetic Constants for the Pseudofirst-Order and Pseudosecond-Order Models

adsorbent	$Q_{e,exp}$ $mg \cdot g^{-1}$	C_0 $mg \cdot L^{-1}$	pseudofirst-order			pseudosecond-order					
			$Q_{e,cal}$ $mg \cdot g^{-1}$	k_1 min^{-1}	R^2	$Q_{e,cal}$ $mg \cdot g^{-1}$	k_2 $g \cdot mg^{-1} \cdot min^{-1}$	h	R^2	$t^{1/2}$	E_a
MIP	13.09	100	5.792	0.00352	0.9623	13.33	0.001981	0.3523	0.9570	37.85	17.08
	18.01	150	10.22	0.00408	0.9834	18.52	0.001149	0.3940	0.9983	47.00	
	23.09	200	12.41	0.00431	0.9511	23.81	0.001010	0.5727	0.9991	41.57	
NIP	10.38	100	4.970	0.00464	0.9690	10.57	0.002837	0.3169	0.9990	33.35	23.88
	12.44	150	5.035	0.00468	0.9529	12.63	0.003104	0.4948	0.9995	25.52	
	16.99	200	6.954	0.00524	0.9283	17.26	0.002498	0.7442	0.9995	23.19	

Table 3. Thermodynamic Parameters for the Adsorption of 3-CP onto MIP and NIP

adsorbent	T/K	thermodynamic parameters		
		ΔG° $kJ \cdot mol^{-1}$	ΔH° $kJ \cdot mol^{-1}$	ΔS° $J \cdot mol^{-1} \cdot K^{-1}$
MIP	298	2.376		
	318	2.986	-6.714	-30.504
	338	3.596		
NIP	298	3.220		
	318	3.887	-6.725	-33.372
	338	4.554		

The K_d and Q_{max} values were calculated to be $96.99 \text{ mg} \cdot \text{L}^{-1}$ and $172.7 \text{ mg} \cdot \text{g}^{-1}$ of dry polymer, respectively. The binding of 3-CP to the NIP was also analyzed by the Scatchard equation (Figure 4b). The linear regression equation of the curve was $Q/[3\text{-CP}] = -0.00627Q + 0.86535$. It revealed homogeneous binding sites with K_d and Q_{max} values of $159.5 \text{ mg} \cdot \text{L}^{-1}$ and $138.01 \text{ mg} \cdot \text{g}^{-1}$, respectively.

Adsorption Kinetic Studies. Adsorption kinetics describe the rate of adsorbate adsorption by a sorbent that control the equilibrium time. Hence, it was investigated for a better understanding of the dynamics of 3-CP adsorption by MIP. The kinetic data obtained were analyzed using a pseudofirst-order rate equation and pseudosecond-order rate equation. The pseudofirst-order expression and pseudosecond-order kinetic model is given as follows:^{25,26}

$$\ln(Q_e - Q_t) = \ln Q_e - k_1 t \quad (9)$$

$$\frac{t}{Q_t} = \frac{1}{k_2 Q_e^2} + \frac{t}{Q_e} \quad (10)$$

where Q_e ($\text{mg} \cdot \text{g}^{-1}$) and Q_t ($\text{mg} \cdot \text{g}^{-1}$) are the amounts of 3-CP adsorbed at equilibrium and at time t , respectively, k_1 is the pseudofirst-order rate constant (min^{-1}), and k_2 is the rate constant of pseudosecond-order adsorption ($\text{g} \cdot \text{mg}^{-1} \cdot \text{min}^{-1}$). Plots of $\ln(Q_e - Q_t)$ versus t give the slope k_1 and intercept $\ln Q_e$. The linear plot of t/Q_t versus t gave $1/Q_e$ as the slope and $1/k_2 Q_e^2$ as the intercept.

On the basis of the pseudosecond-order rate equation, the initial adsorption rate and half adsorption time are estimated by

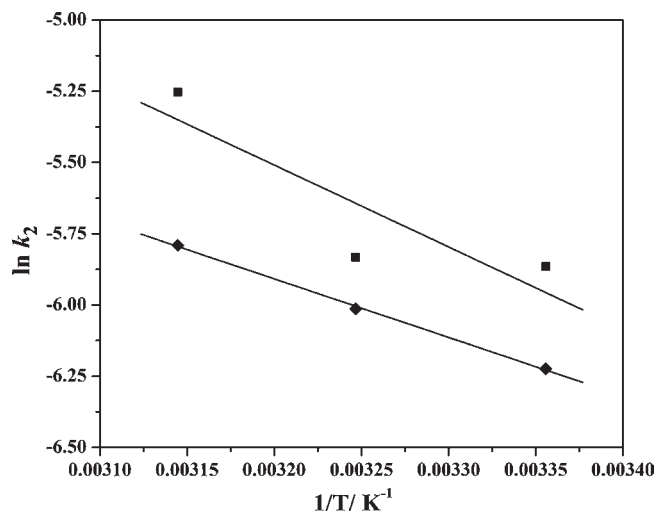


Figure 7. Plots of $\ln k_2$ against $1/T$ for 3-CP adsorption onto (a) MIP and (b) NIP. ■, NIP; ◆, MIP.

the following equations:^{27,28}

$$h = k_2 Q_e^2 \quad (11)$$

$$t_{1/2} = \frac{1}{k_2 Q_e} \quad (12)$$

The half adsorption time $t_{1/2}$ is another parameter and is defined as the time required for the adsorption to take up half as much 3-CP as its equilibrium value. Thus, the initial adsorption rate and half adsorption time are usually applied as a measure of the adsorption rate.

As shown in Figure 5, for MIP, 3-CP uptake increased sharply in the initial stage and then became slow until equilibrium. In addition, the equilibrium concentration increases with an increase of initial concentration. This phenomenon may due to the fact that, initially, all active sites on the MIP composite surface were vacant and the solution concentration was high enough.²⁹ After that period, few active sites were available, and the solution concentration decreased; hence 3-CP uptake became very slow until equilibrium.

The intraparticle diffusion model can be written as follows:³⁰

$$Q_t = k_i t^{1/2} + C \quad (13)$$

where k_i is the intraparticle diffusion rate constant ($\text{mg} \cdot \text{g}^{-1} \cdot \text{min}^{-1/2}$). The value of C ($\text{mg} \cdot \text{g}^{-1}$) and k_i can be

Table 4. Distribution Coefficient and Selectivity Coefficient Data for MIP and NIP

phenolic compounds	MIP			NIP			
	C_e	K_d	k	C_e	K_d	k	k'
	$\text{mg}\cdot\text{L}^{-1}$	$\text{L}\cdot\text{g}^{-1}$		$\text{mg}\cdot\text{L}^{-1}$	$\text{L}\cdot\text{g}^{-1}$		
3-CP	23.19	1.656	-	59.98	0.334	-	-
2,6-CP	53.62	0.432	3.829	56.98	0.377	0.884	4.331
2,4,6-CP	62.90	0.295	5.616	61.69	0.310	1.074	5.229

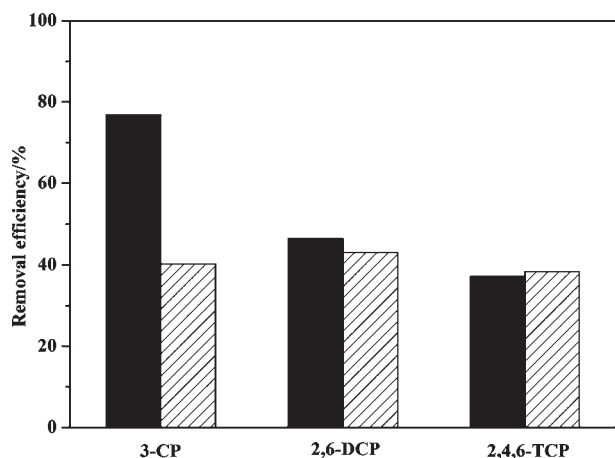


Figure 8. Selectivity of MIP and NIP. Solid column for MIP; Slash column for NIP.

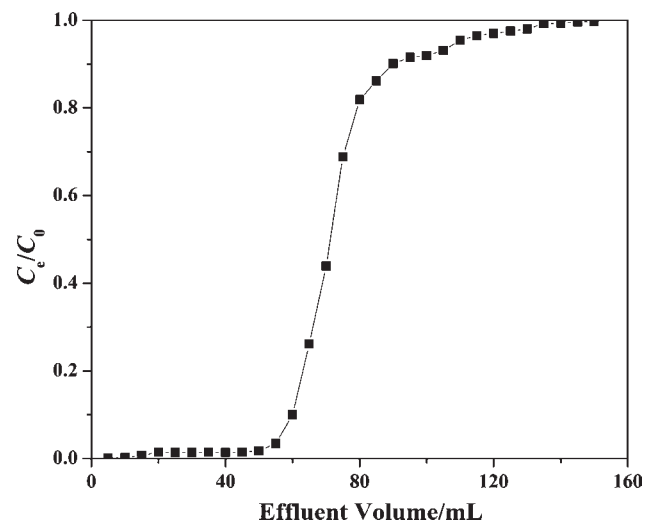


Figure 9. Breakthrough curve of MIP.

evaluated from the intercept and slope of the linear plot of Q_e versus $t^{1/2}$, respectively.

For intraparticle diffusion plots, the first stage (sharper region) is the instantaneous adsorption or external surface adsorption. The second step is the gradual adsorption stage where intraparticle diffusion is rate-limiting. In some cases, a third stage exists, which is the final equilibrium stage where intraparticle diffusion starts to slow down due to the extremely low adsorbate concentrations left in the solutions and the decrease of adsorption sites.^{31,32} Referring to Figure 6, for all initial concentrations, the

first stage was completed within the first 10 min, and the second stage was then attained; finally the third stage occurred. The different stages of the adsorption rates observed indicated that the adsorption rate was initially faster and then slowed down as the time increased. Moreover, the calculated intraparticle diffusion rate constant k_i , shown in Table 2, demonstrated that the intraparticle diffusion rate increases with the increasing initial 3-CP concentration in solution. This indicated that diffusion and adsorption rates were closely related with the concentration gradient.

All of the parameters of the pseudofirst-order, pseudosecond-order, and intraparticle diffusion models are listed in Table 2. From Table 2, the pseudosecond-order equation provided the best coefficients of determination R^2 and the agreement between $Q_{e,cal}$ and $Q_{e,exp}$ was good, whereas the pseudofirst-order and intraparticle diffusion equations do not give a good fit to the experimental data. This suggested that chemical adsorption may be the rate limiting step.

Thermodynamic Study. Thermodynamic parameters such as changes in the standard Gibbs energy (ΔG°), enthalpy (ΔH°), and entropy (ΔS°) can be calculated using the following equations:³³

$$\ln\left(\frac{Q_e}{C_e}\right) = \frac{\Delta S^\circ}{R} - \frac{\Delta H^\circ}{RT} \quad (14)$$

$$\Delta G^\circ = \Delta H^\circ - T\Delta S^\circ \quad (15)$$

where R is the universal gas constant ($8.314 \text{ J}\cdot\text{K}^{-1}\cdot\text{mol}^{-1}$), T is the temperature in Kelvin, and Q_e ($\text{mmol}\cdot\text{g}^{-1}$) and C_e ($\text{mmol}\cdot\text{L}^{-1}$) are the adsorption capacity and concentration at equilibrium, respectively. The values of ΔH° and ΔS° were calculated from the slope and intercept of a van't Hoff plot ($\ln(Q_e/C_e)$ vs $1/T$) as shown in Table 3.

All positive values of ΔG° at various temperatures imply that the adsorption process of 3-CP onto MIP was thermodynamically unfavorable within the temperature range evaluated, while the negative values for ΔS° reflect a decrease in the randomness in the solid–solution interface during the adsorption of 3-CP. When the temperature increases from 25 °C to 45 °C, the magnitude of the Gibbs energy change, ΔG° , shifts to high positive values which suggests that the adsorption was more unfavorable at high temperature. In fact, the negative value of ΔH° indicated that the adsorption of 3-CP onto MIP is exothermic, so decreasing temperature supplies a more favorable adsorption of 3-CP and MIP. The thermodynamic parameters are actually helpful in the practical application of the process.

Moreover, the pseudosecond-order rate constant was also used to estimate the activation energy (E_a , $\text{kJ}\cdot\text{mol}^{-1}$) between

3-CP and the sorbent by the Arrhenius equation:

$$\ln k_2 = \ln A - \frac{E_a}{RT} \quad (16)$$

where E_a is the Arrhenius activation energy of sorption, representing the minimum energy reactants must have for the reaction to proceed, A is the Arrhenius factor, R is the universal gas constant ($8.314 \text{ J} \cdot \text{K}^{-1} \cdot \text{mol}^{-1}$), T is the solution temperature. $-E_a/R$ can be obtained from the slope of a plot $\ln k_2$ versus $1/T$. Chemisorption or physisorption mechanisms are often an important indicator to describe the type of interaction between 3-CP molecules and MIP composites. Generally, low activation energies [$(5 \text{ to } 40) \text{ kJ} \cdot \text{mol}^{-1}$] are characteristic of physisorption, while higher activation energies [$(40 \text{ to } 800) \text{ kJ} \cdot \text{mol}^{-1}$] suggest chemisorption.^{34,35} The value of E_a (Table 2, Figure 7) in this study was $23.88 \text{ kJ} \cdot \text{mol}^{-1}$ (NIP) and $17.08 \text{ kJ} \cdot \text{mol}^{-1}$ (MIP) which indicates that the process was a physical mechanism.

Adsorption Specificity. To investigate the binding specificity of the polymers, an experiment was carried out for the binding of 3-CP, 2,6-DCP, and 2,4,6-TCP (Figure 8), and distribution coefficient and selectivity coefficient data for MIP are given in Table 4.

It can be seen from Figure 8 that the MIP exhibited good adsorption selectivity for the template (3-CP). The adsorption capacity of MIP binding of 3-CP was much higher than that of 2,4-DCP and 2,4,6-TCP. In the adsorption process, many specific artificial recognition sites with respect to template molecules were generated on the surface of MIP, so the template molecules can strongly bind to polymer particles. As competitive molecules, 2,4-DCP and 2,4,6-TCP molecules are small enough to get into the imprinting cavities, but the recognition sites of the imprinting cavities are not complementary to them, so they had less chance to be adsorbed onto the MIP. Hence, the adsorption capacity of the MIP to the two molecules was much lower than that of the template 3-CP molecules. In contrast, the NIP adsorbed the template much less than that of MIP, since NIP had not generated specific recognition sites due to the absence of template molecules during the synthetic process.³⁶

Dynamic and Breakthrough Studies. The dynamic capacity was obtained by pumping $1.0 \text{ g} \cdot \text{L}^{-1}$ of 3-CP solution at pH 7.0 through the column at a flow rate of $1.0 \text{ mL} \cdot \text{min}^{-1}$, then collecting continuously each 5 mL of column effluent to determine the concentration until a saturation value was achieved. For column operation, breakthrough capacity is more significant and useful than the dynamic capacity in application of SPE as it gives an actual working capacity of the sorbent in the column.³⁷ The breakthrough capacity represents the exhaustion point in terms of feed volume, after which the adsorbate leaks through into the effluent in gradually increasing amounts. The leaking volume of 3-CP was 60 mL (Figure 9), and the leaking capacity was $756.8 \text{ mg} \cdot \text{g}^{-1}$. The leaking and the saturated adsorption amounts of 3-CP are $756.8 \text{ mg} \cdot \text{g}^{-1}$ and $1137.58 \text{ mg} \cdot \text{g}^{-1}$, respectively. With regard to the elution, 5 mL of methanol was enough, and the enrichment multiple was 30. Besides, the elution experiment results show that MIP has a fine elution property by using methanol solution as the eluting agent, giving excellent reusability.

CONCLUSION

In this work, a surface molecularly imprinted polymer was developed for the selective extraction of 3-CP from aqueous solution. The optimum pH condition for the adsorption of 3-CP

from aqueous solution was found to be 7.0, which is close to the pH of drinking water. The obtained Arrhenius activation energy E_a of the adsorption indicates that the process was a physisorption mechanism. The selectivity studies suggested that the MIPs exhibit excellent selective recognition for 3-CP when compared with NIPs. Moreover, the total dynamic capacity of MIP was calculated to be $1137.58 \text{ mg} \cdot \text{g}^{-1}$. The 3-CP breakthrough column started after 60 mL, and the breakthrough capacity was $756.8 \text{ mg} \cdot \text{g}^{-1}$. The experimental results obtained in this work show that surface molecularly imprinted polymers can be used for the selective removal of 3-CP from aqueous solutions, and it also demonstrated the potential of molecularly imprinted solid phase extraction.

AUTHOR INFORMATION

Corresponding Author

*Tel.: +86-0511-88790683; fax: +86-0511-88791800. E-mail address: yys@ujs.edu.cn (Y. S. Yan).

Funding Sources

This work was financially supported by the National Natural Science Foundation of China (No. 21077046, No. 30970309), Ph.D. Programs Foundation of Ministry of Education of China (No. 20093227110015), and Ph.D. Innovation Programs Foundation of Jiangsu Province. (No. CX10B_276Z).

REFERENCES

- (1) Rawajfeh, Z.; Nsour, N. Characteristics of phenol and chlorinated phenols sorption onto surfactant-modified bentonite. Molecularly imprinted polymer as micro-solid phase extraction combined with high performance liquid chromatography to determine phenolic compounds in environmental water samples. *J. Colloid Interface Sci.* **2006**, *298*, 39–49.
- (2) Anirudhan, T. S.; Ramachandran, M. Adsorptive removal of tannin from aqueous solutions by cationic surfactant-modified bentonite clay. *J. Colloid Interface Sci.* **2006**, *299*, 116–124.
- (3) Lua, A. C.; Jia, Q. P. Adsorption of phenol by oil-palm-shell activated carbons in a fixed bed. *Chem. Eng. J.* **2009**, *150*, 455–461.
- (4) Park, K. H.; Balathanigaimani, M. S.; Shim, W. G.; Lee, J. W.; Moon, H. Adsorption characteristics of phenol on novel corn grain-based activated carbons. *Microporous Mesoporous Mater.* **2010**, *127*, 1–8.
- (5) Gomez, M.; Matafonova, G.; Gomez, J. L.; Batoev, V.; Christofi, N. Comparison of alternative treatments for 4-chlorophenol removal from aqueous solutions: Use of free and immobilized soybean peroxidase and KrCl excilamp. *J. Hazard. Mater.* **2009**, *169*, 46–51.
- (6) Feng, Q. Z.; Zhao, L. X.; Lin, J. M. Molecularly imprinted polymer as micro-solid phase extraction combined with high performance liquid chromatography to determine phenolic compounds in environmental water samples. *Anal. Chim. Acta* **2009**, *650*, 70–76.
- (7) Duya, S. V.; Lefebvre-Tourniera, L. I.; Pichonb, V.; Hugon-Chapuis, F.; Puya, J. Y.; Périgauda, C. Molecularly imprinted polymer for analysis of zidovudine and stavudine in human serum by liquid chromatography-mass spectrometry. *J. Chromatogr., B* **2009**, *877*, 1101–1108.
- (8) Pradhan, S.; Boopathi, M.; Kumar, O.; Baghel, A.; Pandey, P.; Mahato, T. H.; Singh, B.; Vijayaraghavan, R. Molecularly imprinted nanopatterns for the recognition of biological warfare agent ricin. *Biosens. Bioelectron.* **2009**, *25*, 592–598.
- (9) Chen, L. G.; Zhang, X. P.; Xu, Y.; Du, X. B.; Sun, X.; Sun, L.; Wang, H.; Zhao, Q.; Yu, A.; Zhang, H. Q.; Ding, L. Determination of fluoroquinolone antibiotics in environmental water samples based on magnetic molecularly imprinted polymer extraction followed by liquid chromatography–tandem mass spectrometry. *Anal. Chim. Acta* **2010**, *662*, 31–38.

- (10) Bunte, G.; Hürttlen, J.; Pontius, H.; Hartlieb, K.; Krause, H. Gas phase detection of explosives such as 2,4,6-trinitrotoluene by molecularly imprinted polymers. *Anal. Chim. Acta* **2007**, *591*, 49–56.
- (11) Li, Y.; Li, X.; Li, Y. Q.; Qi, J. Y.; Bian, J.; Yuan, Y. X. Selective removal of 2,4-dichlorophenol from contaminated water using non-covalent imprinted microspheres. *Environ. Pollut.* **2009**, *157*, 1879–1885.
- (12) Caro, E.; Marcé, R. M.; Cormack, P. A. G.; Sherrington, D. C.; Borrell, F. On-line solid-phase extraction with molecularly imprinted polymers to selectively extract substituted 4-chlorophenols and 4-nitrophenol from water. *J. Chromatogr., A* **2003**, *995*, 233–238.
- (13) Sanbe, H.; Haginaka, J. Uniformly sized molecularly imprinted polymers for bisphenol A and β -estradiol: retention and molecular recognition properties in hydro-organic mobile phases. *J. Pharm. Biomed. Anal.* **2002**, *30*, 1835–1844.
- (14) Liu, Y. Q.; Hoshina, K.; Haginaka, J. Monodispersed, molecularly imprinted polymers for cinchonidine by precipitation polymerization. *Talanta* **2010**, *80*, 1713–1718.
- (15) Celiz, M. D.; Aga, D. S.; Colón, L. A. Evaluation of a molecularly imprinted polymer for the isolation/enrichment of β -estradiol. *Microchem. J.* **2009**, *92*, 174–179.
- (16) Sun, Z.; Schüssler, W.; Sengl, M.; Niessner, R.; Knopp, D. Selective trace analysis of diclofenac in surface and wastewater samples using solid-phase extraction with a new molecularly imprinted polymer. *Anal. Chim. Acta* **2008**, *620*, 73–81.
- (17) Baggiani, C.; Baravalle, P.; Giovannoli, C.; Anfossi, L.; Giraudi, G. Molecularly imprinted polymers for corticosteroids: Analysis of binding selectivity. *Biosens. Bioelectron.* **2010**, *26*, 590–595.
- (18) Hu, Y. L.; Li, Y. W.; Liu, R. J.; Tan, W.; Li, G. K. Magnetic molecularly imprinted polymer beads prepared by microwave heating for selective enrichment of agonists in pork and pig liver samples. *Talanta* **2011**, *84*, 462–470.
- (19) Alkaram, U. F.; Mukhlis, A. A.; Al-Dujaili, A. H. The removal of phenol from aqueous solutions by adsorption using surfactant-modified bentonite and kaolinite. *J. Hazard. Mater.* **2009**, *169*, 324–332.
- (20) Senturk, H. S.; Ozdes, D.; Gundogdu, A.; Duran, C.; Soylak, M. Removal of phenol from aqueous solutions by adsorption onto organomodified Tirebolu bentonite: Equilibrium, kinetic and thermodynamic study. *J. Hazard. Mater.* **2009**, *172*, 353–362.
- (21) Li, Q.; Yue, Q. Y.; Su, Y.; Gao, B. Y.; Sun, H. J. Equilibrium, thermodynamics and process design to minimize adsorbent amount for the adsorption of acid dyes onto cationic polymer-loaded bentonite. *Chem. Eng. J.* **2010**, *158*, 489–497.
- (22) Greluk, M.; Hubicki, Z. Kinetics, isotherm and thermodynamic studies of Reactive Black 5 removal by acid acrylic resins. *Chem. Eng. J.* **2010**, *162*, 919–926.
- (23) Zheng, H.; Wang, Y.; Zheng, Y.; Zhang, H. M.; Liang, S. P.; Long, M. Equilibrium, kinetic and thermodynamic studies on the sorption of 4-hydroxyphenol on Cr-bentonite. *Chem. Eng. J.* **2008**, *143*, 117–123.
- (24) Gao, B. J.; An, F. Q.; Zhu, Y. Novel surface ionic imprinting materials prepared via couple grafting of polymer and ionic imprinting on surfaces of silica gel particles. *Polymer* **2007**, *48*, 2288–2297.
- (25) Abramian, L.; El-Rassy, H. Adsorption kinetics and thermodynamics of azo-dye Orange II onto highly porous titania aerogel. *Chem. Eng. J.* **2009**, *150*, 403–410.
- (26) Zhang, Z. Y.; Zhang, Z. B.; Fernández, Y.; Menéndez, J. A.; Niu, H.; Peng, J. H.; Zhang, L. B.; Guo, S. H. Adsorption isotherms and kinetics of methylene blue on a low-cost adsorbent recovered from a spent catalyst of vinyl acetate synthesis. *Appl. Surf. Sci.* **2010**, *256*, 2569–2576.
- (27) Wu, Z. J.; Joo, H.; Lee, K. Kinetics and thermodynamics of the organic dye adsorption on the mesoporous hybrid xerogel. *Chem. Eng. J.* **2005**, *112*, 227–236.
- (28) Han, R. P.; Han, P.; Cai, Z. H.; Zhao, Z. H.; Tang, M. S. Kinetics and isotherms of Neutral Red adsorption on peanut husk. *J. Environ. Sci.* **2008**, *20*, 1035–1041.
- (29) Han, R. P.; Zhang, J. J.; Han, P.; Wang, Y. F.; Zhao, Z. H.; Tang, M. S. Study of equilibrium, kinetic and thermodynamic parameters about methylene blue adsorption onto natural zeolite. *Chem. Eng. J.* **2009**, *145*, 496–504.
- (30) Mezenner, N. Y.; Bensmaili, A. Kinetics and thermodynamic study of phosphate adsorption on iron hydroxide-eggshell waste. *Chem. Eng. J.* **2009**, *147*, 87–96.
- (31) Ofomaja, A. E. Intraparticle diffusion process for lead(II) biosorption onto mansonia wood sawdust. *Bioresour. Technol.* **2010**, *101*, 5868–5876.
- (32) Tan, I. A. W.; Ahmad, A. L.; Hameed, B. H. Adsorption isotherms, kinetics, thermodynamics and desorption studies of 2,4,6-trichlorophenol on oil palm empty fruit bunch-based activated carbon. *J. Hazard. Mater.* **2009**, *164*, 473–482.
- (33) Bayramoglu, G.; Altintas, B.; Arica, M. Y. Adsorption kinetics and thermodynamic parameters of cationic dyes from aqueous solutions by using a new strong cation-exchange resin. *Chem. Eng. J.* **2009**, *152*, 339–346.
- (34) Hasan, M.; Ahmad, A. L.; Hameed, B. H. Adsorption of reactive dye onto cross-linked chitosan/oil palm ash composite beads. *Chem. Eng. J.* **2008**, *136*, 164–172.
- (35) Nollet, H.; Roels, M.; Lutgen, P.; Meeren, P. V.; Verstraete, W. Removal of PCBs from wastewater using fly ash. *Chemosphere* **2003**, *53*, 655–665.
- (36) Zhang, W.; Qina, L.; He, X. W.; Li, W. Y.; Zhang, Y. K. Novel surface modified molecularly imprinted polymer using acryloyl- β -cyclodextrin and acrylamide as monomers for selective recognition of lysozyme in aqueous solution. *J. Chromatogr., A* **2009**, *1216*, 4560–4567.
- (37) Lin, C. R.; Wang, H. Q.; Wang, Y. Y.; Cheng, Z. Q. Selective solid-phase extraction of trace thorium(IV) using surface-grafted Th(IV)-imprinted polymers with pyrazole derivative. *Talanta* **2010**, *81*, 30–36.